CASL-U-2014-0114-000

Power uprates
and plant life extension

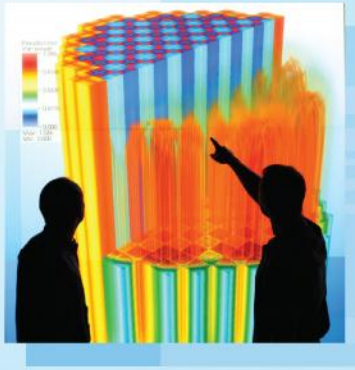

Engineering design
and analysis

Science-enabling
high performance
computing

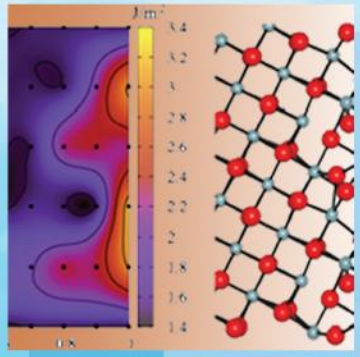

Fundamental science

Plant operational data

Consortium for Advanced Simulation of LWRs

ORIGEN Integration into MPACT

Revision 0
July 4, 2014

Brendan Kochunas
William A. Wieselquist
Ang Zhu

U.S. DEPARTMENT OF ENERGY | Nuclear Energy

REVISION LOG

Revision	Date	Affected Pages	Revision Description
0	7/4/2014	All	Initial version

Document pages that are:

Export Controlled None

IP/Proprietary/NDA Controlled None

Sensitive Controlled None

Requested Distribution:

To: N/A

Copy: N/A

EXECUTIVE SUMMARY

This report documents the work performed to meet the objectives of the RTM milestone on ORIGEN Integration into MPACT. The main objective of the milestone was to demonstrate the capability to perform depletion problems with MPACT where the point depletion calculation, which solves the nuclide transmutation equation with ORIGEN. While MPACT already has a depletion capability based on ORIGEN [4], it is desired to transition to using ORIGEN because ORIGEN has undergone far more validation and software quality assurance than the implementation in MPACT.

The integration was completed by compiling and linking the two codes together at build-time. Within the TriBITS build structure used for VERA, the MPACT and SCALE code repositories are already present. An optional dependency was created between MPACT to SCALE. The API available within ORIGEN was modified slightly to be able to be used by MPACT and two new software classes were implemented in MPACT to call the necessary ORIGEN subroutines.

To test the ORIGEN integration two benchmark problems were analyzed. The first being the spent fuel isotopics from the Takahama-3 PWR reactor. This involved comparisons to experimentally measured nuclide concentrations for select actinides and fission products, and comparisons to other numerical results. The benchmark defines a 1-D problem limiting most of the effects due to the accuracy of a multi-dimensional transport solver, and thus differences can be assumed to be more likely caused by the point depletion solver methodology and associated nuclear data.

The other benchmark analyzed two problems from the reactor physics benchmarks for LWR next generation fuel. The two configurations simulated were a PWR UO_2 pin cell and PWR UO_2 assembly.

For all the benchmark problems the results were generally in good agreement with the other numerical results which were computed by several codes, including MPACT with its original depletion implementation documented in [4]. Thus it is concluded that ORIGEN was successfully integrated into MPACT and is capable of providing reasonable results.

An additional cursory analysis of the performance of the ORIGEN point depletion compared to native MPACT point depletion solver was also performed. In this analysis it was observed that ORIGEN, on average, needs about 0.28 to 0.30 seconds to perform the point depletion calculation. This is greater than the target performance of 0.1 seconds which means future work to investigate smaller depletion chains will be needed. The MPACT internal depletion solver completes the point depletion calculation in 0.02 seconds, so it may be used for routine analysis until the use of a simplified burnup chain and performance improvements are implemented.

Other future work should focus on implementing the post-correction fix-up and quadratic depletion and computation of decay heat and gamma sources.

TABLE OF CONTENTS

REVISION LOG ii

EXECUTIVE SUMMARY iii

TABLE OF CONTENTS v

FIGURES vi

TABLES vi

ACRONYMS vii

1. Introduction 1

2. ORIGEN API Integration 2
- 2.0 Overview of MPACT Infrastructure for Depletion 2
- 2.1 Existing ORIGEN API 7
- 2.2 Integration of the ORIGEN API 8

3. Analysis of Takahama-3 Spent Fuel Isotopics 10
- 3.0 Overview 10
- 3.1 Analysis Methodology and Problem Modeling 10
- 3.2 Results 12
- 3.3 Discussion of Results 18

4. Analysis of Reactor Physics Benchmarks Suite for LWR Next Generation Fuels 19
- 4.0 Overview 19
- 4.1 Summary of Problem Description and Modeling 19
- 4.2 Results & Discussion 21

5. Conclusions 25

REFERENCES 26

FIGURES

Figure 1. Depletion Solution Algorithm [3] 3
Figure 2. UML Legend 4
Figure 3. Software Design for MPACT Depletion Implementation 4
Figure 4. UML Class Diagram of CLASS(DepletionBaseType) 6
Figure 5. UML Class Diagram of CLASS(PointDepletion_Base) 6
Figure 6. Software Design for MPACT Depletion with ORIGEN API integrated 9
Figure 7. NT3G23 Measurement Locations for SF95 (A-Q) and SF96 (C-M) [6] 10
Figure 8. NT3G24 Measurement Location for SF97 (I-Q) [6] 10
Figure 9. Axial Measurement Locations of SF95 Fuel Rod [6] 11
Figure 10. Axial Measurement Locations of SF97 Fuel Rod [6] 11
Figure 11. Averaged C/E Results for SF95 Measurement Locations 12
Figure 12. Averaged C/E Results for SF97 Measurement Locations 13
Figure 13. Schematic view of the fuel pin cell [2] 19
Figure 14. Geometric configuration of PWR UO_2 fuel assembly [2] 20
Figure 15. UO_2 pin k-infinity 22
Figure 16. UO_2 pin Δk comparisons 22
Figure 17. Comparison of k-infinity to average value for UO2 Assembly 23
Figure 18. UO_2 assembly peaking factor 23

TABLES

Table 1 Analytic measurement techniques and uncertainty [1] 11
Table 2. Average of Results for SF95 14
Table 3. Average of Results for SF97 16
Table 4. Component Run times for PWR Assembly Problem in serial 24
Table 5. Component Run times for PWR Assembly Problem with 4 threads 24

ACRONYMS

1D	One-Dimensional
2D	Two-Dimensional
API	Application Program Interface
CASL	Consortium for Advanced Simulation of Light Water Reactors
MG	Multi-group (as in cross sections)
MPACT	Michigan Parallel Characteristics Transport Code
ODE	Ordinary Differential Equation
ORIGEN	ORNL Isotope Generation and Depletion Code
ORNL	Oak Ridge National Laboratory
QA	Quality Assurance
UM	University of Michigan
UML	Unified Modeling Language

1. INTRODUCTION

The main reactor core simulator in the Consortium for Advanced Simulation of Light Water Reactors (CASL) is the MPACT (Michigan PArallel Characteristics Transport Code) code originally developed at the University of Michigan and now jointly developed by UM and ORNL. The key characteristics of the MPACT code include the subgroup method and the embedded self-shielding method (ESSM) for resonance treatment, a whole core solver with a 2-D (MOC)/1-D (Nodal-Diffusion) synthesis method, and the matrix exponential method for burnup based on the SCALE-ORIGEN solver.

The available depletion solver for the matrix exponential method in MPACT is based on the one in ORIGEN. However, unlike ORIGEN it uses a simplified 510 nuclide chain, that has not been extensively validated or quality assured. Although there are several new methods to obtain a solution for the matrix exponential burnup equation, the ORIGEN solver has probably undergone the most extensive verification and validation of any depletion tool currently available. Therefore, it is believed that ORIGEN is sufficiently accurate and robust enough to be applied to reactor applications of interest to CASL.

ORIGEN also provides various other functionalities that may be useful in future applications and could provide an overall increase in value for the CASL core simulator. In particular, ORIGEN is also capable of calculating delayed gamma and decay heat source terms; two features needed for a more accurate simulation of the reactor heat source.

The objective of this milestone is to integrate the ORIGEN API into the existing infrastructure for depletion in MPACT and demonstrate the new depletion capability on a few test problems.

This following section of the report describes the work done to integrate ORIGEN into MPACT. Section 3 presents the analysis of the first test problem, the Takahama-3 benchmark [1], and section 4 presents the analysis of the Benchmark Suite for Reactor Physics Study of LWR Next Generation fuels [2]. Section 5 provides a discussion of areas of future work. Section 6 is the conclusions.

Contributors to this report include (in alphabetical order):

- Ben Collins, ORNL (formerly UM)
- Jess Gehin, ORNL
- Daniel Jabaay, UM
- Kang-Seog Kim, ORNL
- Brendan Kochunas, UM
- William Wieselquist, ORNL
- Ang Zhu, UM

2. ORIGEN API INTEGRATION

2.0 Overview of MPACT Infrastructure for Depletion

The existing depletion implementation in MPACT is based largely on previous work [3]. However, several key changes to the high level software design were made in porting the code to MPACT. The high level software design and algorithms used in the MPACT implementation are the focus of this section.

The software and algorithm conceptualize the depletion calculation into essentially three distinct parts: the point depletion calculation, the transport calculation, and the time stepping algorithm. One could distinguish the transport calculation into two parts: the resonance calculation and transport calculation, but for simplicity these are grouped together.

The point depletion calculation is the heart of the depletion capability. It is responsible for solving the differential equation for nuclide transmutation by radioactive decay and nuclear reaction in each discrete spatial region and is given as:

$$\frac{dN_i(t)}{dt} = \sum_{j=1} \ell_{ij} \lambda_j N_j + \bar{\phi} \sum_{k=1} f_{ik} \sigma_{t,k} N_k - (\lambda_i + \sigma_{a,i} \bar{\phi}) N_i \qquad \text{Eq. (2.1)}$$

where

- $N_i(t)$: particle number density of nuclide i
- λ_i : the radioactive disintegration constant for nuclide i
- $\sigma_{a,i}$: the effective 1-group neutron absorption cross section of nuclide i
- $\sigma_{t,k}$: the effective 1-group total neutron cross section of nuclide k
- $\bar{\phi}$: the total neutron scalar flux
- l_{ij} : the fractions of radioactive disintegrations by nuclide j which lead to the formation of nuclide i
- f_{ik} : the fractions of neutron reactions by nuclide k which lead to the formation of nuclide i.

The details of the MPACT implementation of the point depletion calculation are omitted here for brevity, but can be found in [4]. The functionalized form for the point depletion computational kernel is given as

$$\vec{N}(\Delta t) = F_{\text{POINT-DEPLETION}}\left(\bar{\phi}, \vec{\sigma}, \vec{N}_0, \Delta t\right) \qquad \text{Eq. (2.2)}$$

where $\vec{N}_0$ is the vector of all the initial nuclide concentrations in a given discrete spatial region, $\bar{\phi}$ is the local scalar flux spectrum normalized to the total power, $\vec{\sigma}$ is vector of all microscopic cross sections for all nuclides and reactions evaluated at the regions local conditions, Δt is the time of exposure.

The transport calculation is essentially providing a solution to the Boltzmann transport equation to provide the scalar flux used in Eq. 2.1. This scalar flux along with the multi-group cross sections are used to provide the absorption and total cross sections in 2.1. It is important to note that in the solution for at power conditions this will also involve thermal-hydraulic feedback that must be accounted for in the solution process.

The piece then that resides "above" the point depletion calculation and transport calculation is the time stepping algorithm. The time stepping algorithm can be thought of as an abstract numerical evaluation; in other words it just determines the order of function evaluations, it does not define the method by which the function is evaluated. The concrete time-stepping method implemented in MPACT is the predictor-corrector method, the details of which are also described in [4] as well. Figure 1 below describes the overall predictor-corrector algorithm currently implemented.

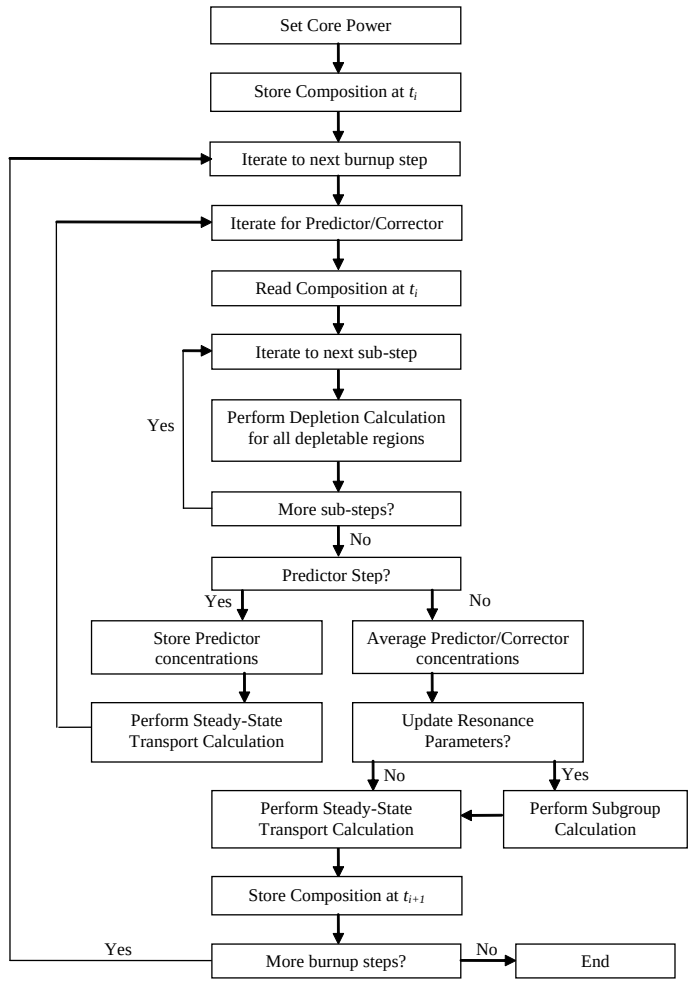

Figure 1. Depletion Solution Algorithm [3]

Based on the mental model described so far, the corresponding high level software design that was developed is shown in Figure 3. Figure 3 is known as a UML class diagram, which is a type of diagram frequently used to illustrate features of software. A short key for the meaning of the diagram objects in Figures 3 through 5 is given in Figure 2.

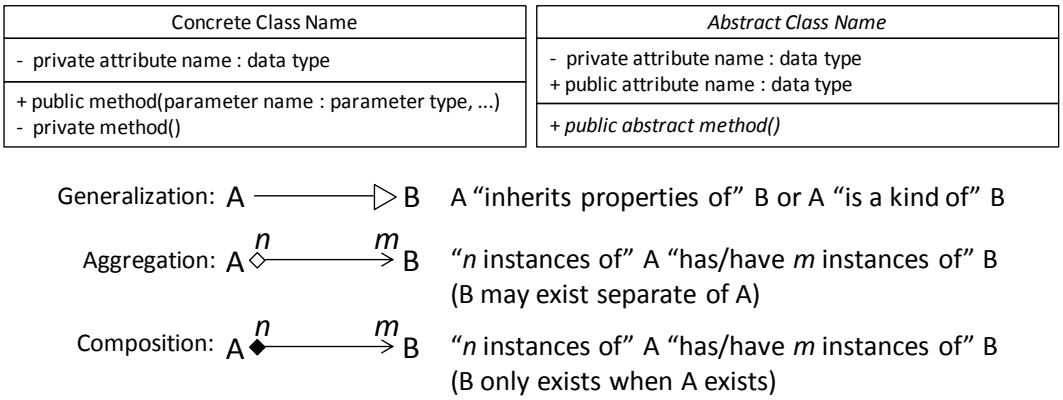

Figure 2. UML Legend

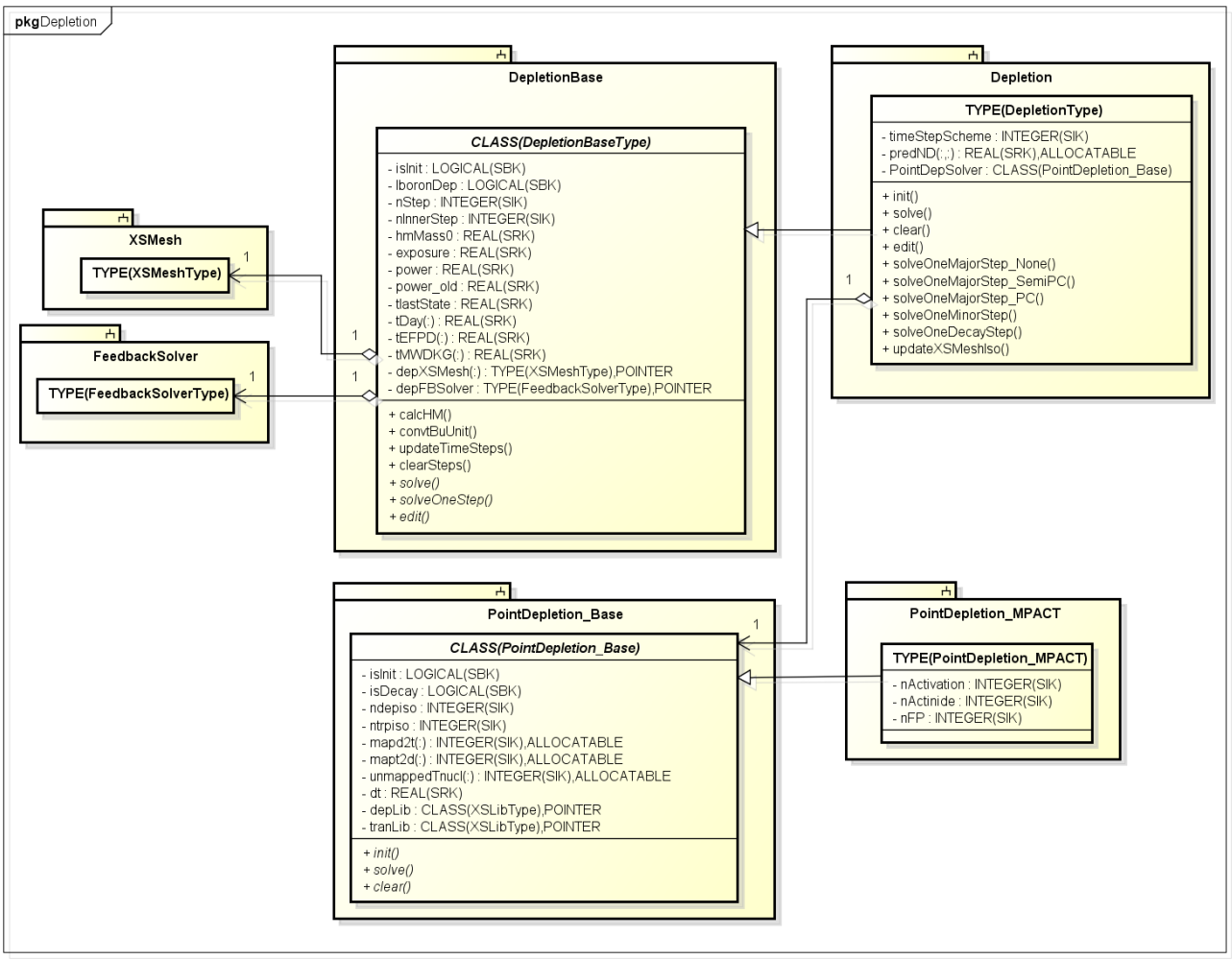

Figure 3. Software Design for MPACT Depletion Implementation

This figure indicates several key components and their function within the system can be inferred from the UML. In plain English though the Figure 3 illustrates the following:

1. The definition of an *abstract class*, `CLASS(PointDepletion_Base)`, for a point depletion solver. As an abstract class this object only defines the minimum data required for this object and the interfaces for any procedures related to the objects operations. For any concrete implementation these translate to requirements for that implementation.
    a. The data require index mapping arrays between nuclides in the cross section library used by the transport solver and nuclides in a supplemental depletion cross section library that defines the decay chains and provides additional data (e.g. decay rates and decay reaction ratios). It also requires pointers to the two libraries.
    b. The *methods* (procedures) defined include initialization (`init`), destruction (`clear`) and `solve`.
2. The definition of an *abstract class* for a depletion algorithm
    a. This defines the required data as being the initial heavy metal mass of the core, power of the current state and previous state, the time steps in various units of exposure, pointers to the cross section mesh and steady state eigenvalue solver with feedback, and dimension info.
    b. The methods include calculation of the heavy metal mass, unit conversion between various units of burnup, solve and edit.
3. A concrete implementation of a point depletion solver, `TYPE(PointDepletion_MPACT)`
    a. This is the implementation of the point depletion solver documented in [4].
4. A concrete implementation of a depletion algorithm, `TYPE(DepletionType)`
    a. This object implements the algorithm depicted in Figure 1.

Figures 4 and 5 below provide more detailed information about the abstract base classes. Particularly the arguments of the defined interfaces.

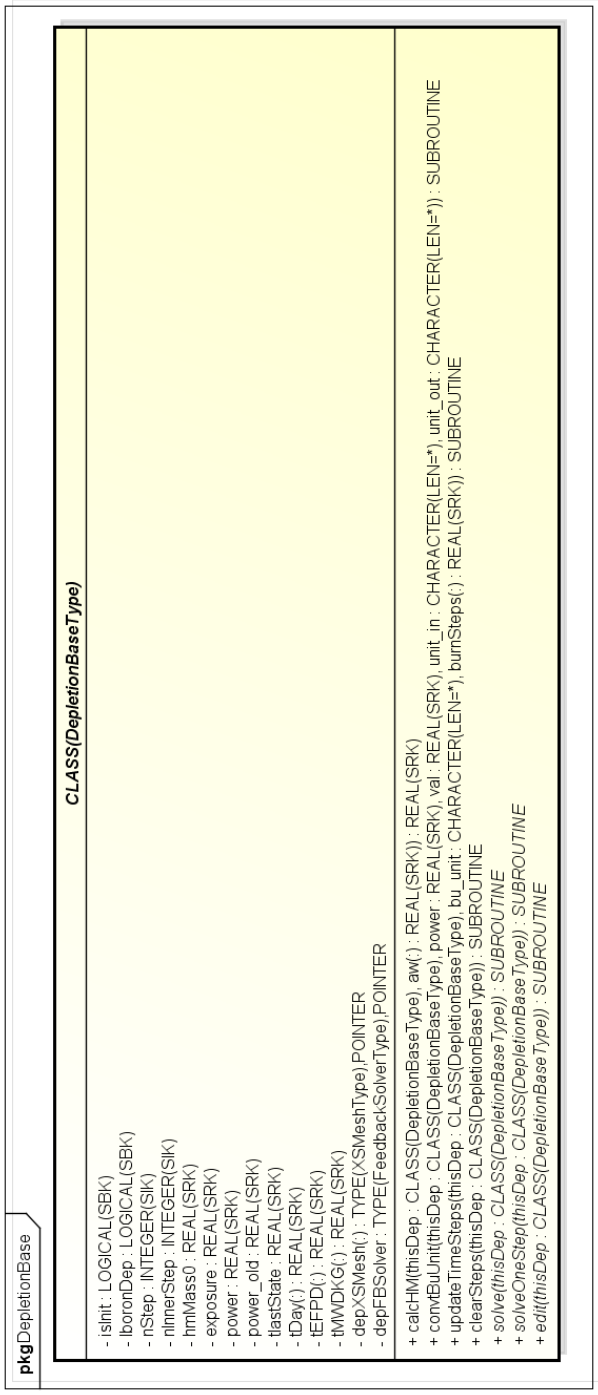

Figure 4. UML Class Diagram of `CLASS(DepletionBaseType)`

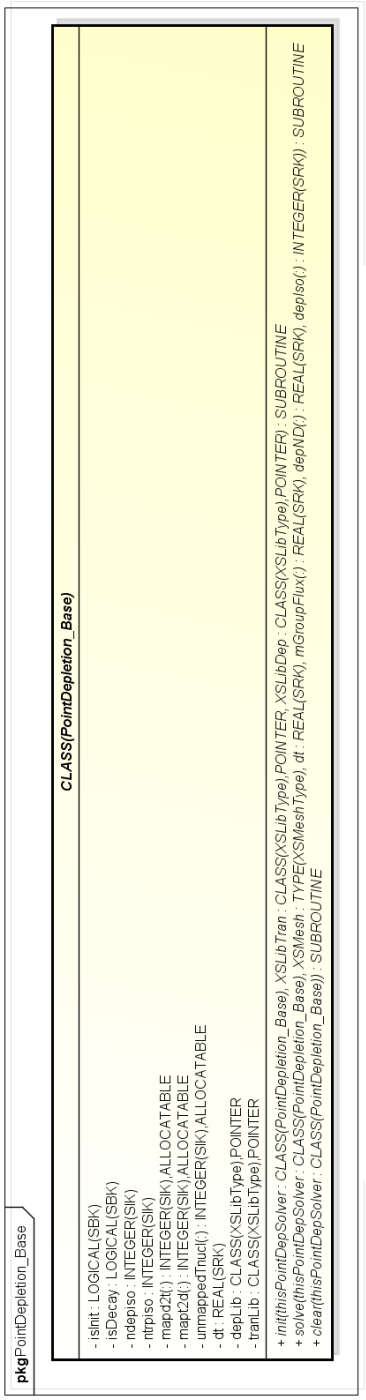

Figure 5. UML Class Diagram of `CLASS(PointDepletion_Base)`

Note that since abstract classes exist for each of the components, it facilitates the use of additional implementations for point depletion solvers and depletion algorithms. This is important because, as will be described in the section 2.2, the integration of ORIGEN will make use of this design feature to provide a different concrete implementation of `CLASS(PointDepletion_Base)`, while making use of the existing depletion algorithm; thus minimizing duplication of effort and maximizing code reuse.

2.1 Existing ORIGEN API

The ORIGEN API, which is itself a collection of APIs, began in earnest in 2012 with a rewrite of ORIGEN's data container classes as object-oriented C++ with Fortran bindings. As of mid-year 2014, the ORIGEN API provides the following capabilities.

- Read/write ORIGEN data files including: fission yields, decay data, and alpha, beta, gamma emission data. Also the ability to create ORIGEN "libraries", basically transition matrices (see Eq. 2.1) as a function of burnup and potentially more parameters, e.g. assembly enrichment.
- Interpolate transition matrices on burnup, enrichment, etc. to perform accurate isotopic depletion/decay calculations without coupling to a transport solver for a set of pre-calculated assembly designs.
- Solve the equations with the ORIGEN matrix exponential solver. Also includes some external solvers such as Radau5 and a Runge-Kutta method. The external solvers are not well-tested.
- Perform alpha, beta, gamma emission calculations.
- Convert concentrations to/from a large set of units, e.g. activity (Ci) to mass (g) or mass (g) to decay heat (W).
- Build new or update existing transition matrices on-the-fly for the purposes of coupling to transport codes.

APIs addressing the first five capabilities were completed by mid-2013, allowed coupling of ORIGEN to Shift (a Monte Carlo code) and Polaris (a lattice physics code). The APIs also allowed rapid development of new ORIGEN front ends: ORIGAMI for assembly irradiation calculations and ORIGEN-GUI, a new graphical user interface. However, the last bullet, the fully in-memory API for multi-group cross section collapse and on-the-fly updating of the ORIGEN transition matrix, a capability provided by external SCALE module COUPLE, was not available until early 2014 in a prototype. From the perspective of transport code coupling, there are two basic components.

1. **Origen_TransitionMatrixUpdater**, responsible for collapsing multi-group fluxes and cross-sections and producing new transition matrices. The main class methods are listed below.
    - **get_concentrations()** – get concentrations at all times**load –** loads decay, multi-group auxiliary library, and fission product yields from files
    - **update_mg_flux –** update internal 1-group xs based on new flux (basically an update of the infinitely dilute xs)
    - **update_user_xs** – update specific 1-group xs provided by the user
    - **update_absorption_fission_xs** – update 1-group xs based on fission and absorption xs provided by the user (useful when these are the only self-shielded xs)
    - **get_transition_matrix()** – get the current (updated) transition matrix
2. **Origen_Case**, responsible for receiving initial number densities, a transition matrix, time step, power/flux level, and calculation options and producing end-of-step number densities. The main class methods are listed below.
    - **set_time –** sets the time steps
    - **set_flux –** sets the total flux over each time step
    - **set_transition_matrix** – sets the transition matrix
    - **set_conc0()** – set concentrations at t=0

2.2 Integration of the ORIGEN API

The use of abstract base classes in MPACT greatly facilitates the integration of the ORIGEN API. There are basically two main classes that need to be implemented in MPACT for ORIGEN integration: **PointDepletionOrigenType** and **XSLibType_Origen**.

Shown below in Figure 6 is the brief UML for the ORIGEN API-based depletion and MPACT native depletion, showing only the relevant data members and methods.

- The blue boxes represent the two classes that must be implemented.
- The orange boxes represent ORIGEN API classes.
- The green boxes are MPACT classes that will be used without modification. They include interfaces for the depletion solver (DepletionBaseType on the left), which includes predictor/corrector capability and substepping, as well as the ODE solver class interface (PointDepletionBaseType) responsible for each substep solve, and the XSLibType base data interface class.
- The yellow boxes represent components of the native MPACT depletion scheme that will not be modified.

A. **PointDepletionOrigenType** – This will be the concrete *solver* class for ORIGEN depletion calculations, implementing **init**, **solve**, and **clear** methods. PointDepletionOrigenType will inherit from abstract base class PointDepletionBaseType contained in file MPACT_libs/Depletion/src/PointDepletion_Base.f90. All classes of PointDepletionBaseType contain a pointer to a depletion library (*depLib* member) of type XSLibType. For PointDepletionOrigenType, this will be required to be XSLibType_Origen. The **solve** method creates an Origen_Case (populating time, flux, attaching a transition matrix), run the calculation, and destroy the case.

B. **XSLibType_Origen** – This will be the concrete *data* class for depletion calculations. XSLibType_Origen will inherit from abstract base class XSLibType contained in file MPACT_libs/Reactor/src/XSLibraryType_Base.f90. The **init** method of XSLibType_Origen will be used to load various data from disk. Mandatory data is:

   a. Decay constant and branching ratio data (λ),
   b. Multi-group cross section data for depletion including isomeric branching (σ), and
   c. Energy-dependent fission yield data (γ).

The **init** method creates an Origen_TransitionMatrixUpdater, loading the above pieces of data from files. The methods of the Origen_TransitionMatrixUpdater will be used to construct a problem-dependent transition matrix for each call of PointDepletionOrigenType's **solve**.

Optional data that may be used in the future is:

   d. Recoverable energy data (Q),
   e. Fraction of Q in emitted photons (f_g),
   f. Toxicity factors in air and water (R_{air} & R_{water}), and
   g. Nuclide mass data (m).

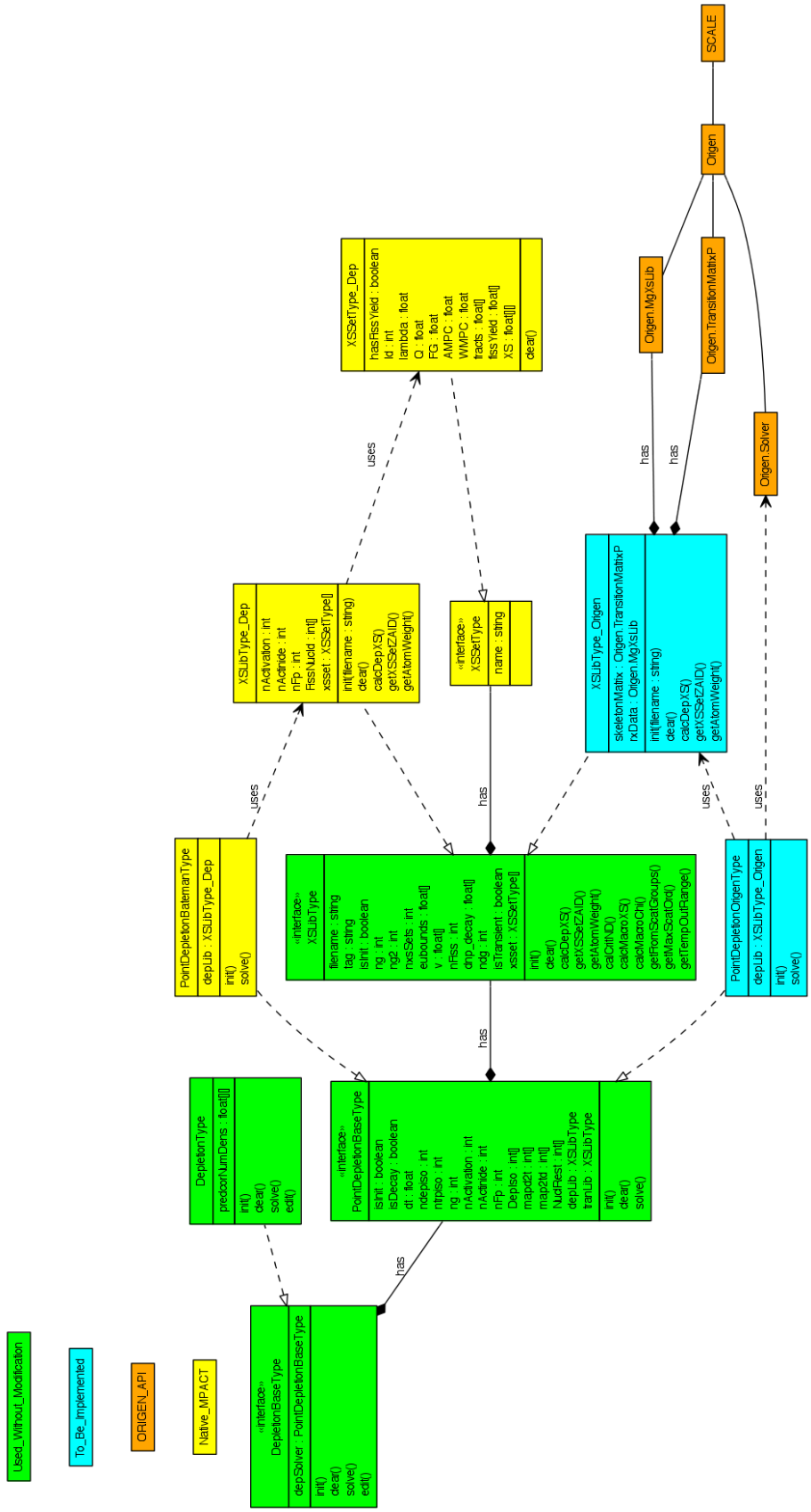

Highlighting ORIGEN API (orange), classes to be implemented (blue), the existing MPACT "native" depletion scheme (yellow), and higher level classes that may be used without modification (green). Note that this is a left-to-right view of the heirarchy, i.e. the highest-level classes are on the left.

Figure 6. Software Design for MPACT Depletion with ORIGEN API integrated

3. ANALYSIS OF TAKAHAMA-3 SPENT FUEL ISOTOPICS

3.0 Overview

To demonstrate the depletion capability and to provide some preliminary validation of the point depletion solver, nuclear data, and its integration into the MPACT code the Takahama-3 benchmark is performed. This problem is included as part of the ORIGEN-S validation base [1], and has been used previously to validate the point depletion solver implemented in MPACT [4]. This problem is chosen for the preliminary validation for several reasons.

- It has been run previously to validate the separate components that are being integrated.
- The problem has reference computational results and experimental measurements allowing for the comparison to numerical and experimental results.
- It defines equivalent 1-D problems for each measurement location, which simplifies the analysis by eliminating other sources of inconsistencies. (e.g. the quality of the 2-D or 3-D spatial solution of the transport problem is less of a concern).
- The data for comparison is the EOL isotopics.

3.1 Analysis Methodology and Problem Modeling

The Takahama-3 benchmark [1] defines the core operating parameters and basic geometry that describe a 2-D assembly. The detailed power histories are given for each of the 16 measurement locations on three fuel rods (SF95, SF96, and SF97), which come from two 17x17 PWR assemblies (NT3G23 and NT3G24) that operated within the Takahama-3 PWR. The original purpose of this benchmark was to validate depletion solvers and their nuclear data for the application to high enrichment and high burnup fuels. Figure 7 through Figure 10 below shows the measurement locations analyzed.

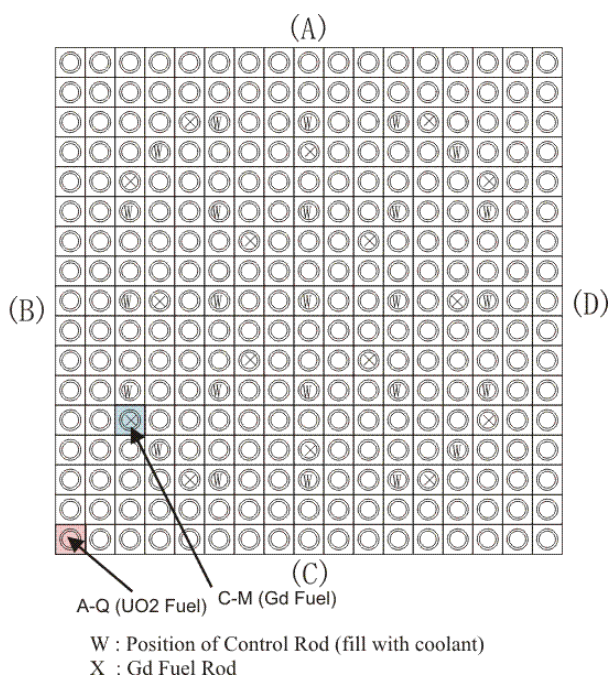

Figure 7. NT3G23 Measurement Locations for SF95 (A-Q) and SF96 (C-M) [6]

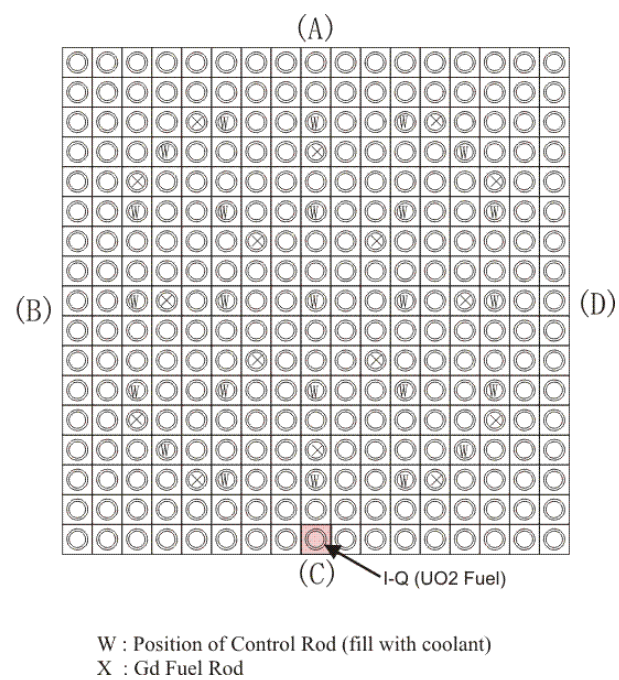

Figure 8. NT3G24 Measurement Location for SF97 (I-Q) [6]

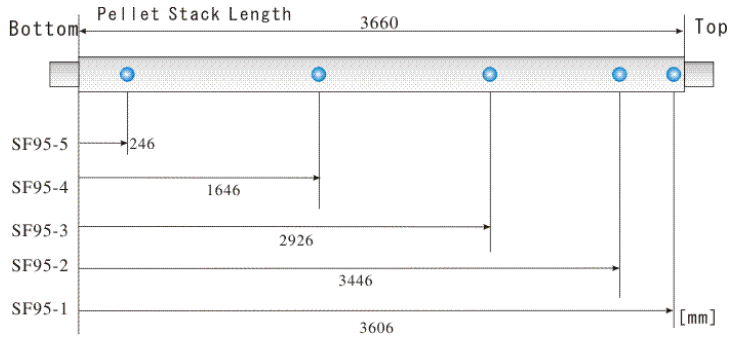

Figure 9. Axial Measurement Locations of SF95 Fuel Rod [6]

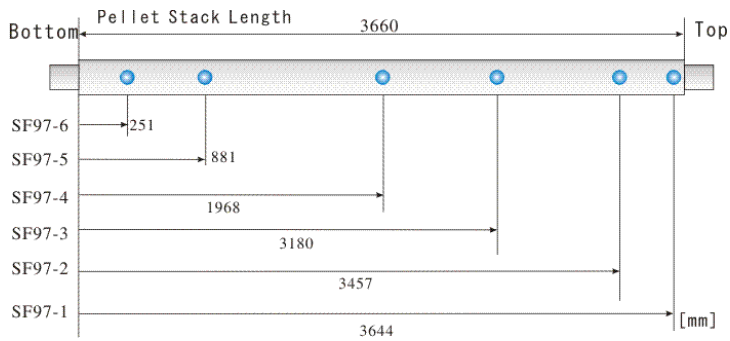

Figure 10. Axial Measurement Locations of SF97 Fuel Rod [6]

The measurement methodology for the experimental results is described in detail in [5]. To summarize, the measurements used gamma spectroscopy in two stages. First non-desctructive γ-ray scans were performed on the individual fuel rods. Then destructive radiochemical analyses were performed. The collected samples were dissolved and measured using α-ray spectroscopy, γ-ray spectroscopy, and mass spectrometry. The error in the measured concentrations of the isotopes varies by the measurement method, isotope, and location. However, the error in the experimental measurements is no greater than 10%. A summary of the measurement error is given in Table 1 below, which is copied from [1]. More detailed discussions of these errors can be found in [5] and [1].

Table 1. Analytic measurement techniques and uncertainty [2]

Nuclide	Measurement Technique	Relative standard deviation
^{234}U	Isotopic dilution mass spectrometry (IDMS)	< 1%
^{235}U, ^{238}U	IDMS	< 0.1%
^{236}U	IDMS	< 2%
^{238}Pu	IDMS	< 0.5%
^{239}Pu, ^{240}Pu, ^{241}Pu, ^{242}Pu	IDMS	< 0.3%
Nd, Sm isotopes	IDMS	< 0.1%
^{241}Am, ^{243}Cm, ^{244}Cm	α-ray spectroscopy, mass spectrometry	< 2%
^{243}Am, ^{246}Cm	α-ray spectroscopy, mass spectrometry	< 5%
^{242m}Am, ^{242}Cm, ^{247}Cm	α-ray spectroscopy, mass spectrometry	< 10%
Gd isotopes	mass spectrometry	< 0.1%
^{237}Np	α-ray spectroscopy	< 10%
^{134}Cs, ^{137}Cs, ^{154}Eu	γ-ray spectroscopy	< 3%
^{106}Ru	γ-ray spectroscopy	< 5%
^{125}Sb, ^{144}Ce	γ-ray spectroscopy	< 10%

The model built in MPACT consisted of a 2-D pin cell with reflective boundary conditions that preserves the overall fuel to moderator ratio of the assembly and uses an estimate of the local T/H conditions. Three rings are used in the fuel where the isotopics are tracked independently. A ray spacing of 0.03 cm was used with the Chebyshev-Yamamoto quadrature having 16 azimuthal angles and 2 polar angles per octant. The convergence criteria were set to 1.e-6. The pin cell was also divided into 8 azimuthal regions for the flux calculation. For the depletion, the transport calculations were performed at every burnup step where the power changed (see [1] for details). Two depletion substeps were performed between successive transport calculations. The simulation was run in serial.

3.2 Results

The comparison of the rod averaged results are given in Table 2 and Table 3 which show the C/E values for the EOL number densities of various actinides and fission products for which measurements were taken by gamma scans. The SF96 cases were not simulated because of the difficulty in developing a 1-D model that properly accounts for the local heterogeneity of the pin containing gadolinium burnable poison surrounded by regular UO_2 fuel pins. The SAS2H and HELIOS results are taken from [1]. The DeCART results come from [3]; these are included since the MPACT implementation is based on the DeCART implementation. The MPACT results come from [4], and the MPACT+ORIGEN results were computed as part of the work of this milestone.

Figure 11 and 12 below show the same data given in Tables 2 and 3. averages and standard deviations over all measurement locations.

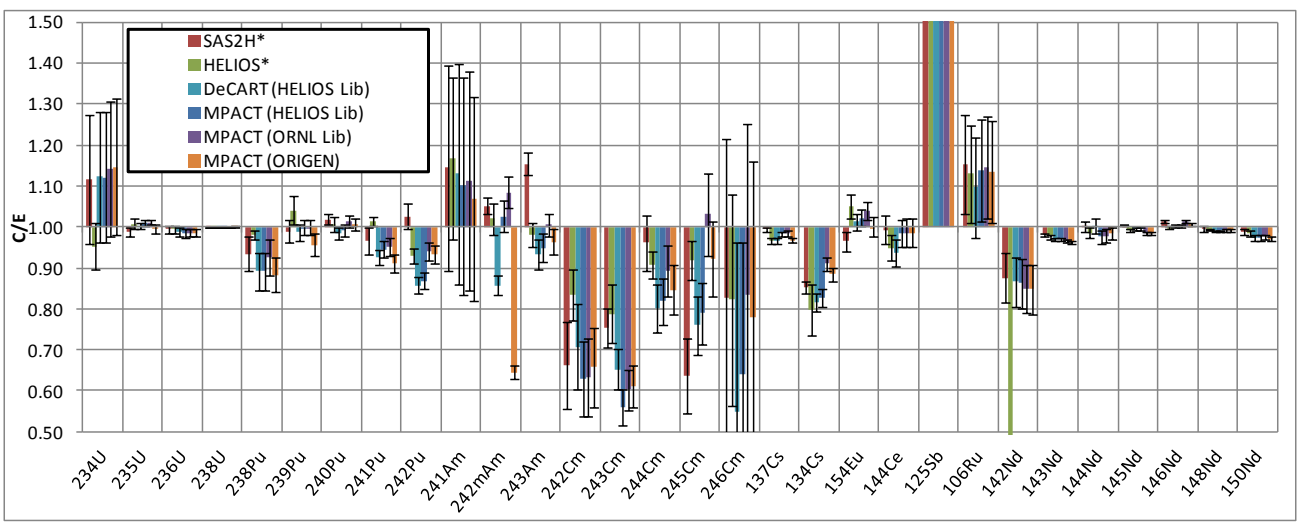

Figure 11. Averaged C/E Results for SF95 Measurement Locations

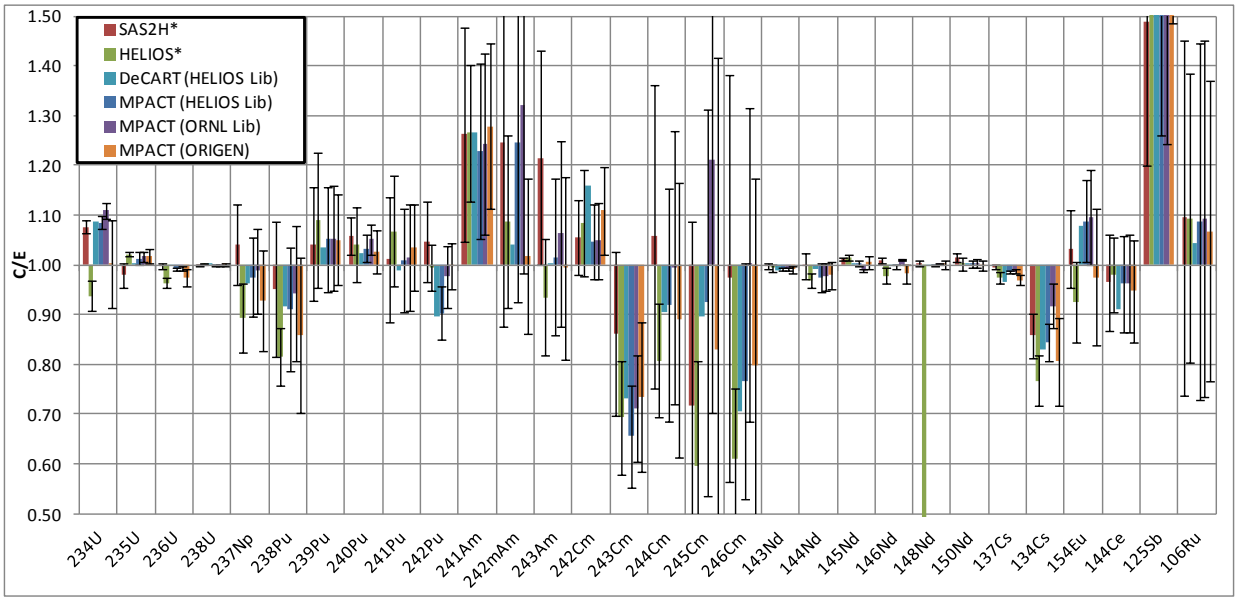

Figure 12. Averaged C/E Results for SF97 Measurement Locations

Table 2. Average of Results for SF95 (1/2)

Isotope	SAS2H		HELIOS		DeCART		MPACT (HELIOS)		MPACT (ORNL)		MACT+ORIGEN	
	Average C/E	Std. Dev.	Average C/E	Std. Dev.	Average C/E	Std. Dev.	Average C/E	Std. Dev.	Average C/E	Std. Dev.	Average C/E	Std. Dev.
^{234}U	1.12	0.16	0.95	0.06	1.12	0.16	1.12	0.16	1.14	0.16	1.15	0.17
^{235}U	0.99	0.01	1.01	0.01	1.00	0.01	1.01	0.01	1.01	0.01	0.99	0.01
^{236}U	0.99	0.01	0.99	0.01	0.99	0.01	0.98	0.01	0.99	0.01	0.99	0.01
^{238}U	1.00	0.00	1.00	0.00	1.00	0.00	1.00	0.00	1.00	0.00	1.00	0.00
^{238}Pu	0.93	0.04	0.98	0.01	0.89	0.04	0.89	0.04	0.93	0.04	0.88	0.04
^{239}Pu	0.99	0.03	1.04	0.03	0.99	0.02	1.00	0.02	1.00	0.02	0.96	0.03
^{240}Pu	1.02	0.01	1.01	0.02	0.98	0.01	0.99	0.01	1.01	0.01	1.01	0.01
^{241}Pu	0.97	0.03	1.01	0.01	0.93	0.02	0.94	0.02	0.95	0.02	0.91	0.02
^{242}Pu	1.03	0.03	0.93	0.02	0.86	0.02	0.87	0.02	0.94	0.02	0.93	0.02
^{241}Am	1.14	0.25	1.17	0.20	1.13	0.27	1.10	0.27	1.11	0.27	1.07	0.25
^{242m}Am	1.05	0.02	1.02	0.04	0.86	0.02	1.03	0.04	1.08	0.04	0.65	0.01
^{243}Am	1.15	0.03	0.98	0.03	0.93	0.04	0.95	0.03	1.00	0.03	0.96	0.03
^{242}Cm	0.66	0.11	0.83	0.06	0.71	0.10	0.63	0.09	0.63	0.09	0.66	0.10
^{243}Cm	0.75	0.05	0.79	0.07	0.65	0.05	0.56	0.04	0.60	0.05	0.61	0.05
^{244}Cm	0.96	0.07	0.91	0.03	0.80	0.06	0.82	0.06	0.89	0.06	0.85	0.06

Table 2. Average of Results for SF95 (2/2)

Isotope	SAS2H		HELIOS		DeCART		MPACT (HELIOS)		MPACT (ORNL)		MACT+ORIGEN	
	Average C/E	Std. Dev.	Average C/E	Std. Dev.	Average C/E	Std. Dev.	Average C/E	Std. Dev.	Average C/E	Std. Dev.	Average C/E	Std. Dev.
^{245}Cm	0.64	0.09	0.92	0.05	0.76	0.07	0.79	0.08	1.03	0.10	0.92	0.09
^{246}Cm	0.83	0.39	0.82	0.26	0.55	0.42	0.64	0.32	0.83	0.42	0.78	0.38
^{137}Cs	0.99	0.01	0.97	0.01	0.96	0.01	0.98	0.01	0.98	0.01	0.97	0.01
^{134}Cs	0.85	0.01	0.80	0.06	0.82	0.02	0.83	0.02	0.91	0.02	0.88	0.02
^{154}Eu	0.96	0.02	1.05	0.03	1.01	0.02	1.02	0.02	1.04	0.02	1.00	0.02
^{144}Ce	0.99	0.03	0.95	0.03	0.94	0.03	0.98	0.03	0.98	0.03	0.98	0.03
^{125}Sb	2.05	0.35	2.65	0.23	2.10	0.35	2.16	0.36	2.13	0.35	2.48	0.40
^{106}Ru	1.15	0.12	1.13	0.12	1.10	0.12	1.14	0.13	1.14	0.12	1.13	0.12
^{142}Nd	0.88	0.06	N/A	N/A	0.87	0.06	0.86	0.06	0.85	0.06	0.85	0.06
^{143}Nd	0.98	0.00	0.98	0.01	0.97	0.00	0.97	0.00	0.97	0.00	0.96	0.00
^{144}Nd	1.00	0.01	0.98	0.01	1.00	0.02	0.98	0.02	0.98	0.02	0.98	0.01
^{145}Nd	1.00	0.00	0.99	0.00	1.00	0.00	0.99	0.00	0.98	0.00	0.98	0.00
^{146}Nd	1.01	0.00	1.00	0.00	1.00	0.00	1.00	0.00	1.01	0.00	1.01	0.00
^{148}Nd	1.00	0.01	0.99	0.00	0.99	0.00	0.99	0.00	0.99	0.00	0.99	0.00
^{150}Nd	0.99	0.01	0.98	0.01	0.97	0.01	0.97	0.01	0.98	0.01	0.97	0.01

Table 3. Average of Results for SF97 (1/2)

Isotope	SAS2H		HELIOS		DeCART		MPACT (HELIOS)		MPACT (ORNL)		MACT+ORIGEN	
	Average C/E	Std. Dev.	Average C/E	Std. Dev.	Average C/E	Std. Dev.	Average C/E	Std. Dev.	Average C/E	Std. Dev.	Average C/E	Std. Dev.
^{234}U	1.08	0.01	0.94	0.03	1.09	0.01	1.09	0.01	1.11	0.02	1.00	0.09
^{235}U	0.98	0.02	1.02	0.01	1.00	0.02	1.01	0.01	1.02	0.01	1.02	0.01
^{236}U	1.00	0.01	0.96	0.01	1.00	0.00	0.99	0.00	0.99	0.00	0.97	0.02
^{238}U	1.00	0.00	1.00	0.00	1.00	0.00	1.00	0.00	1.00	0.00	1.00	0.00
^{238}Pu	1.04	0.08	0.89	0.07	0.96	0.08	0.97	0.08	0.99	0.08	0.93	0.10
^{239}Pu	0.95	0.14	0.82	0.06	0.92	0.12	0.91	0.12	0.94	0.14	0.86	0.16
^{240}Pu	1.04	0.12	1.09	0.14	1.04	0.11	1.05	0.11	1.05	0.11	1.05	0.09
^{241}Pu	1.06	0.04	1.04	0.07	1.02	0.03	1.03	0.03	1.05	0.03	1.03	0.04
^{242}Pu	1.01	0.13	1.07	0.11	0.99	0.10	1.01	0.10	1.02	0.11	1.03	0.09
^{241}Am	1.05	0.08	0.99	0.05	0.90	0.05	0.90	0.05	0.98	0.06	1.00	0.05
^{242m}Am	1.26	0.22	1.27	0.14	1.27	0.19	1.23	0.18	1.24	0.18	1.28	0.17
^{243}Am	1.25	0.37	1.09	0.17	1.04	0.29	1.25	0.32	1.32	0.34	1.02	0.15
^{242}Cm	1.21	0.22	0.94	0.12	1.00	0.15	1.02	0.16	1.06	0.19	0.99	0.18
^{243}Cm	1.06	0.08	1.08	0.11	1.16	0.08	1.05	0.08	1.05	0.08	1.11	0.09
^{244}Cm	0.86	0.17	0.69	0.11	0.73	0.11	0.66	0.10	0.71	0.11	0.74	0.15

Table 3. Average of Results for SF97 (2/2)

Isotope	SAS2H		HELIOS		DeCART		MPACT (HELIOS)		MPACT (ORNL)		MACT+ORIGEN	
	Average C/E	Std. Dev.	Average C/E	Std. Dev.	Average C/E	Std. Dev.	Average C/E	Std. Dev.	Average C/E	Std. Dev.	Average C/E	Std. Dev.
^{245}Cm	1.06	0.30	0.81	0.11	0.91	0.23	0.92	0.23	1.00	0.27	0.89	0.28
^{246}Cm	0.72	0.37	0.60	0.21	0.90	0.37	0.92	0.39	1.21	0.51	0.83	0.59
^{137}Cs	0.97	0.41	0.61	0.14	0.70	0.11	0.77	0.24	1.00	0.32	0.80	0.37
^{134}Cs	1.00	0.01	0.99	0.01	0.99	0.00	0.99	0.00	0.99	0.00	0.99	0.01
^{154}Eu	1.00	0.03	0.97	0.01	0.99	0.03	0.97	0.03	0.98	0.03	0.98	0.03
^{144}Ce	1.01	0.00	1.01	0.01	1.00	0.00	1.00	0.00	0.99	0.00	1.01	0.01
^{125}Sb	1.01	0.00	0.98	0.02	1.00	0.00	1.00	0.00	1.01	0.00	0.98	0.02
^{106}Ru	1.00	0.01	N/A	N/A	1.00	0.00	1.00	0.00	1.00	0.00	1.00	0.01
^{142}Nd	1.01	0.01	1.00	0.01	1.00	0.01	1.00	0.01	1.00	0.01	1.00	0.01
^{143}Nd	1.00	0.00	0.97	0.01	0.97	0.00	0.99	0.00	0.99	0.00	0.97	0.01
^{144}Nd	0.86	0.04	0.77	0.05	0.83	0.04	0.84	0.04	0.92	0.05	0.81	0.09
^{145}Nd	1.03	0.08	0.92	0.08	1.08	0.08	1.09	0.08	1.10	0.10	0.98	0.14
^{146}Nd	0.96	0.10	0.98	0.08	0.91	0.09	0.96	0.10	0.96	0.10	0.95	0.10
^{148}Nd	1.49	0.29	1.82	0.17	1.51	0.29	1.56	0.30	1.53	0.29	1.74	0.25
^{150}Nd	1.09	0.36	1.09	0.29	1.04	0.35	1.09	0.36	1.09	0.36	1.07	0.30

The average time per point depletion solve in these calculations is estimated somewhere around 0.43 seconds. The targeted execution time for the point depletion calculation was previously suggested to be 0.1 seconds, so there is some work to be done to improve performance to reach the target execution time.

3.3 Discussion of Results

In [1] the numerical results for SF95 and SF97 are said to be in "extremely good agreement" with experimental measurement, and compare similarly to "previous isotopic benchmark studies". Overall the *average* results of MPACT+ORIGEN are comparable to the others. This suggests that ORIGEN has been successfully integrated into MPACT, and that MPACT can call ORIGEN to perform the point depletion calculation. Furthermore, the expected results from the point depletion calculation should be in agreement Comparing the results further, it is observed that the most notable differences of the MPACT+ORIGEN are in the prediction of Am-242m in SF95. The average result for this isotope differs significantly from the other simulations and experiment. However, in the SF97 case MPACT+ORIGEN does the best at predicting the Am-242m concentration, albeit the standard deviation for this point is fairly large. The average U-234 concentration is also in notably good agreement with the experimental value, but once again there is a large standard deviation for this data point which suggests this could be the result of a cancellation of errors. The isotopes with the highest standard deviations and C/E values include the higher actinides and some fission products, in particular Sb-125. In the case of the higher actinides (e.g. curium) the numerical results typically under-predict these quantities compared to the experimental measurements, while the concentrations of americium are generally over-predicted. Given that the transmutation paths to higher actinides all involve transmuting through americium, this suggests that the capture and decay to higher actinides from americium is under predicted.

The Am-242m concentration along with the higher actinides, that transmute through Am-242, are very sensitive to the ratio of the (n,γ') reaction to the (n,γ) reaction. This ratio is strongly energy dependent ranging from 10% at low energies to 50% at high energies. In ORIGEN-S at the time of the writing of [1] this ratio was given as 16%. In the MPACT depletion implementation the data specifies this ratio to be around 16.2%. The newer ORIGEN-S data for LWRs gives the ratio around 10%, so this ratio being less, and the observation that the C/E being under-predicted is consistent. Using a typical LWR spectrum to collapse the point-wise data gives a ratio around 16%, however the ratio should be collapsed with the total capture reaction rate, and doing so yields a value close to 10%. Thus, there may still be some debate about what the appropriate value should be, however, some consider a C/E within ±40% for Am-242m to be reasonable.

Since the C/E deviations from 1.0 are generally observable in all the numerical results it suggests the cause may be systematic. Two possibilities that could explain these systematic differences are: that there is a problem in the development of the corresponding 1-D model or there is a problem in the nuclear data. In [1], a 2-D analysis was also done alongside the 1-D analysis verifying that 1-D models used for SF95 and SF97 were appropriate (although this was not the case for the Gd_2O_3 bearing rod SF96, which was not modeled as a part of this work for this reason). This suggests that the 1-D approach is valid for SF95 and SF97 and that the issue is the nuclear data. Because the numerical results encompass a variety of methods and nuclear data, this seems to suggest that there could still be issues with the nuclear data. To address this, future work on modeling a 2-D lattice may be able to provide some insight.

4. ANALYSIS OF REACTOR PHYSICS BENCHMARKS SUITE FOR LWR NEXT GENERATION FUELS

4.0 Overview

To further demonstrate the depletion capability, in particular the ability to simulate problems relevant to CASL, the benchmark suite for reactor physics study of LWR next generation fuels is chosen because the benchmark specifies a range of problems with varying complexity for normal LWR operating conditions. The results for comparison were also generated using a wide range of methods and nuclear data. However, no reference result exists, and the results are only numerical. The benchmark specifies single pin, PWR assembly, and BWR assembly configurations for UO_2 and MOX fuel. The purpose of the benchmark was to assess the methods and data of the reactor physics community at large in their ability to predict the reactivity and isotopics of LWR fuel and assemblies at high burnup (up to 70 GWd/MTU). This suite of benchmark problems was also analyzed in previous work on the depletion capability already implemented in MPACT [5].

4.1 Summary of Problem Description and Modeling

The problems that were chosen to be analyzed for this milestone included the single pin problem and the UO_2 assembly problem as these are the most relevant problems for CASL. The geometric specifications are shown in Figure 13 and Figure 14. The rest of the detailed specifications are omitted here for brevity, but can be readily found in [2].

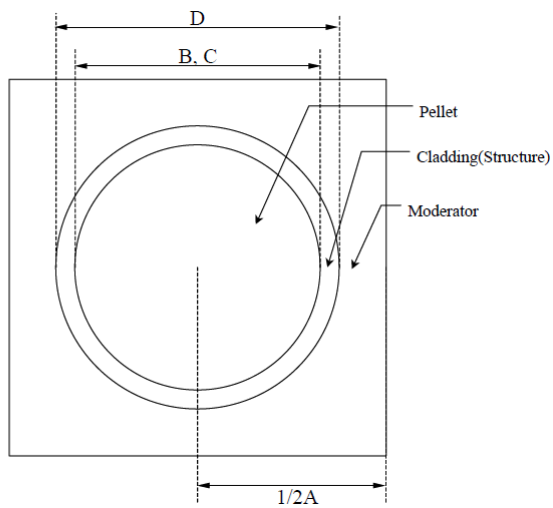

Abbreviation	Description	cm
A	Fuel rod pitch	1.265
B, C	Pellet outer & Cladding inner diameter	0.824
D	Cladding outer diameter	0.952

Figure 13. Schematic view of the fuel pin cell [2]

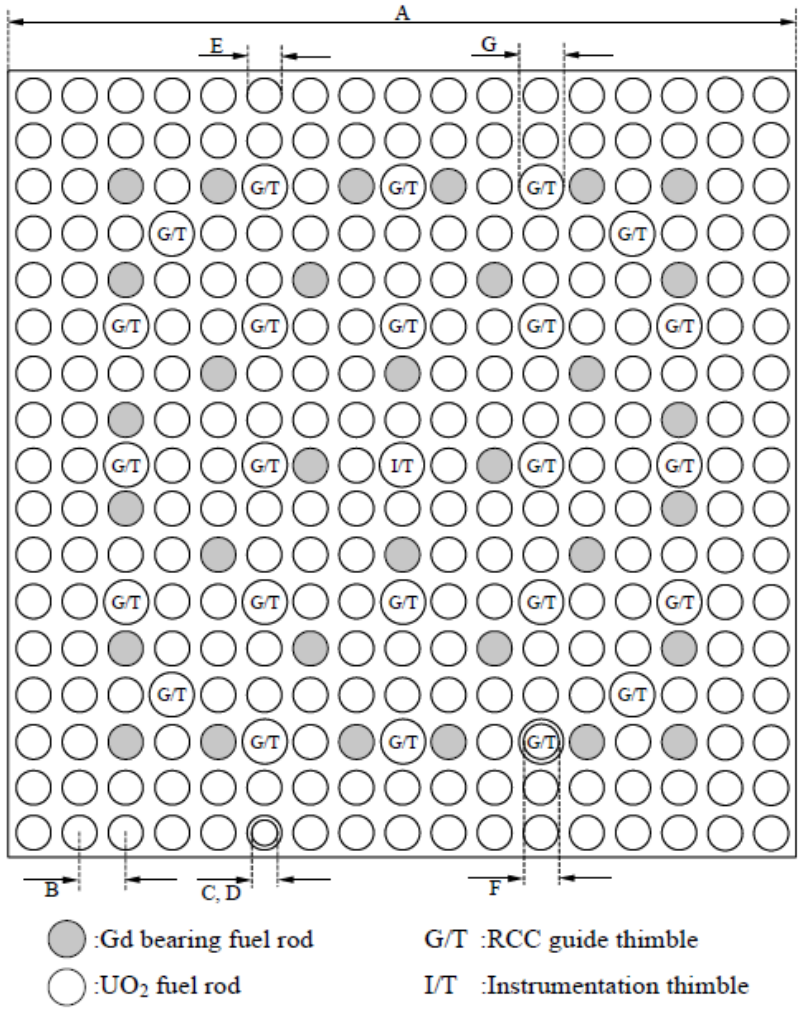

Abbreviation	Description	cm
A	Fuel assembly pitch	21.505
B	Fuel rod pitch	1.265
C, D	Pellet outer & Cladding inner diameter	0.824
E	Cladding outer diameter	0.952
F	I/T, G/T inner diameter	1.140
G	I/T, G/T outer diameter	1.220

Figure 14. Geometric configuration of PWR UO_2 fuel assembly [3]

The PWR UO_2 fuel assembly used in the benchmark here is the same geometrical configuration as a 17x17 type PWR fuel design. The average ^{235}U enrichment is 6.2 wt% assuming 21 effective full power months operation using a three batch loading strategy. The assembly is composed of UO_2 and UO_2-Gd_2O_3 (Gd) fuel rods. The detail information about the geometry can be found in reference [4].

In each model the fuel is meshed with 3 radial rings where isotopes are tracked independently. The pins also have 8 azimuthal divisions for scalar flux. The ray discretization was 16 azimuthal and 3

polar angles in the Chebyshev-Yamamoto product quadrature and a spacing of 0.03 cm. The convergence criteria were set to 1.e-6. For the depletion the predictor-corrector time step method was used. In the assembly problem the transport calculations were performed at 0.1 and 0.5 MWD/kg and then every 1 MWD/kg from 1 MWD/kg to 25 MWD/kg, then every 2.5 MWD/kg up to 70 MWD/kg. In the pin cell problem transport calculations were performed at 0.1 and 0.5 MWD/kg, then every 1 MWD/kg from 1 MWD/kg to 15 MWD/kg, and then every 2.5 MWD/kg from 15 MWD/kg to 70 MWD/kg. In the assembly model four depletion substeps were taken between transport calculations. In the pin cell model two depletion substeps were taken between every transport calculation. The calculations were performed in serial and *no symmetry* was used. The simulations were run on the CASL development workstation u233, which is a shared resource.

4.2 Results & Discussion

The multiplication factor as a function of burnup is compared along with the depleted particle number densities for the major heavy nuclides and fission products at end of life (EOL). In the original benchmark the pin cell cases also included a comparison of reaction rates, but this is omitted in the analysis here. The DeCART result is taken from previous work related to [3] and the MPACT results come from [4]. All the other code solution are from [7,8], with the exception of the MPACT+ORIGEN results which were computed as a part of the work done in this milestone.

Figure 13 shows the k-infinity for the UO_2 pin case. The MPACT results from HELIOS library and ORNL library agree well with the SRAC results; while other code results exist, only the SRAC and average of all participants are included. In [9] it is suggested that the SRAC results are the results that could be considered as the best numerical reference. The SRAC results used nuclear data from the following libraries: JENDL-3.2 (J32), JENDL-3.3 (J33), JEF-2.2 (F22) and ENDF-VI Rev. 5 (B65). The average includes results that used ENDF-IV and ENDF-V nuclear data.

The k-infinity calculated with the ORNL library is consistently about 300-400 pcm smaller than the k-infinity calculated with the HELIOS library (as can be seen in Figure 16). This was not totally unexpected since the ORNL library is generated from ENDF-VII while the HELIOS library is based largely on ENDF-VI data. It should also be noted that the solutions beside MPACT (ORNL) were calculated from a variety of libraries, including. As discussed above, the ENDF version of the ORNL library is different, so there are some isotopes with higher percentage difference of the concentration from ORNL library. The MPACT+ORIGEN results used the ORNL library and are consequently very similar.

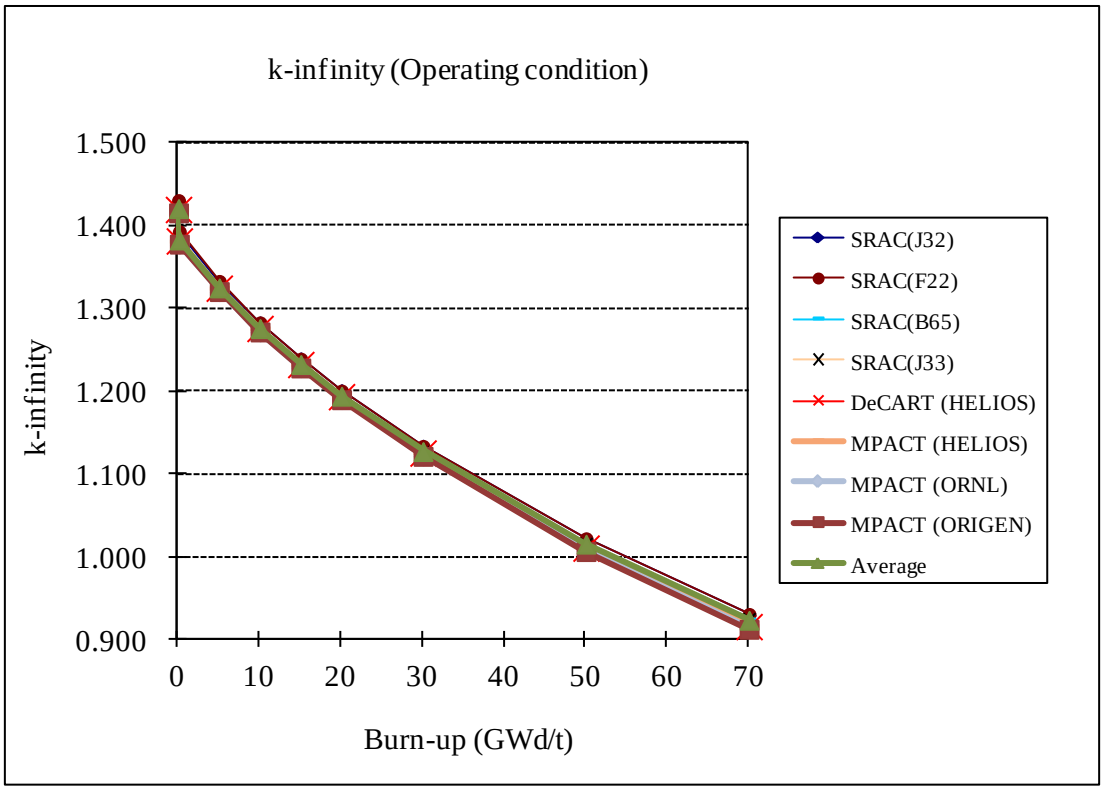

Figure 15. UO_2 pin k-infinity

Figure 16 below shows the k from the average to better highlight some of the differences in the results. All the MPACT results predict a faster loss in reactivity compared to the average, and in particular the ORNL library.

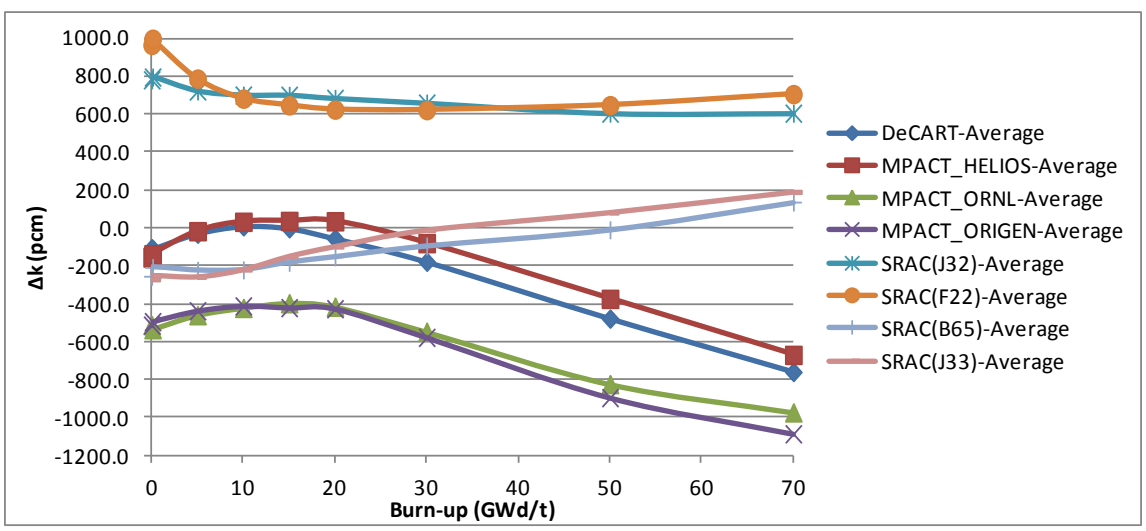

Figure 16. UO_2 pin Δk comparisons

The k-infinite and the pin power peaking factor for the PWR UO_2 fuel assembly are shown in Figure 17 and Figure 18 and good agreement is seen for MPACT with other codes. The ORNL library k-infinite is still 300-400 pcm smaller than HELIOS library consistently, which again is likely due to the version of the ENDF library. The MPACT+ORIGEN result has the most negative burnup reactivity. This could possibly be due to several effects which include: additional fission product poisoning or an over-prediction of the U-235 reaction rate or an under-prediction of U-238

transmuting to Pu-239 and Pu-241. Because the peaking factors in Figure 16 are consistent with the other results, suggesting the relative fission rates between the pins is the same, the overall drop in reactivity is more likely from an effect that does not vary from pin to pin.

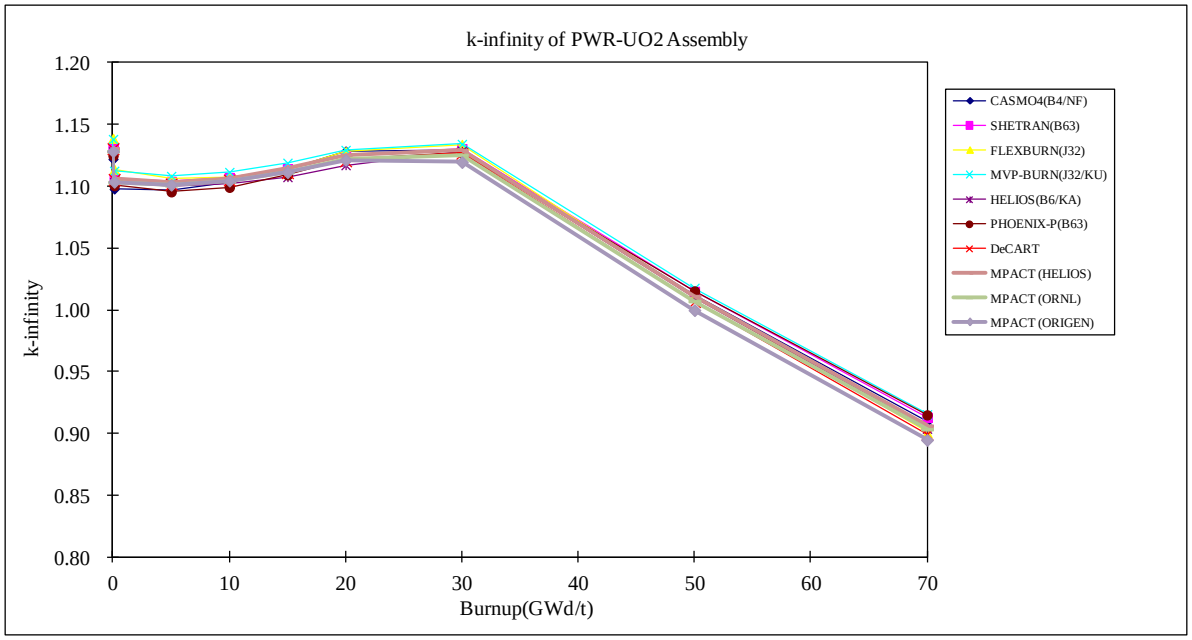

Figure 17. Comparison of k-infinity to average value for UO_2 Assembly

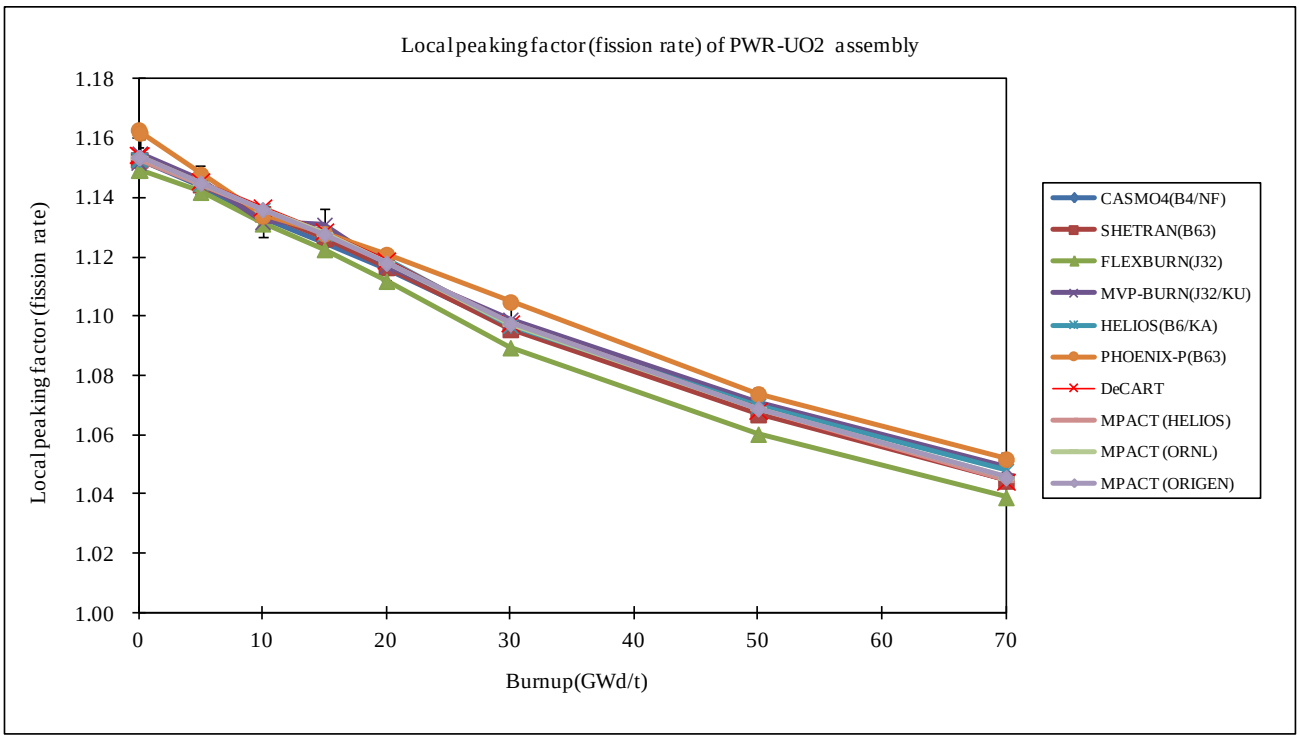

Figure 18. UO_2 assembly peaking factor

In terms of the computational performance of the point depletion calculation, the solver implemented originally in MPACT for [4] does a point depletion calculation, on average, in about 0.02 seconds. This was computed from the JAERI UO_2 pin and UO_2 PWR assembly problems. This execution time is 5x faster than the target execution time for the point depletion solver. For ORIGEN the estimated

time to do a point depletion calculation for these problems is approximately 0.28 to 0.3 seconds. It is important to note that the depletion chain in ORIGEN includes more than 2200 nuclides while MPACT has only 510. One area of future work will be to develop a more optimized depletion chain.

For the UO_2 assembly problem with the internal MPACT point depletion solver, the average time to compute a state-point was about 30 minutes. The total time for 46 states was just over 23 hours. Approximately 86.91% of that time was spent in the MOC calculation (includes subgroup fixed source problem). 3% of the time was spent in CMFD. This leaves about 9.94% of the time that was spent in the depletion calculation. With the ORIGEN point depletion solver approximately 58.79% of the time is spent in depletion. Table 4 below presents the amount of time spent in each computational kernel throughout the entire depletion.

Table 4. Component Run times for PWR Assembly Problem in Serial

Component	MPACT		MPACT+ORIGEN	
	HH:MM:SS	% Total	HH:MM:SS	% Total
MOC (including subgroup)	20:07:51	86.91%	19:56:12	39.70%
CMFD	00:43:53	3.16%	00:45:36	1.51%
Depletion	02:18:05	9.94%	29:31:20	58.79%
Total Solve	23:09:49	100%	50:13:08	100%

The case was also run with 4 threads in the MOC kernel with all other inputs being equal to the serial case. Note again that the platform on which the timing results were taken from was a shared resource so some variability is expected in the results. For the most part though the MOC and CMFD times are consistent between the two cases, with only the time for depletion having a significant difference.

Table 5. Component Run times for PWR Assembly Problem with 4 Threads

Component	MPACT		MPACT+ORIGEN	
	HH:MM:SS	% Total	HH:MM:SS	% Total
MOC (including subgroup)	04:47:22	63.80%	04:49:56	13.17%
CMFD	00:38:51	8.63%	00:41:31	1.89%
Depletion	02:04:10	27.57%	31:10:05	84.94%
Total Solve	07:30:23	100%	36:41:32	100%

5. CONCLUSIONS

The objective of the milestone was to integrate ORIGEN into MPACT so that MPACT can use ORIGEN to perform the point depletion calculation. The integration involved some minor changes to the build systems of MPACT and SCALE and the addition of two new software classes into MPACT. Some other minor changes to the ORIGEN API were also needed.

Two benchmarks with various problems were analyzed to test the integration of ORIGEN into MPACT. The first benchmark, Takahama-3, compared numerical results for a 1-D problem with experimentally measured isotopic concentrations. This benchmark focuses more on the accuracy of the point depletion solver methodology and nuclear data then on the transport solver, since the problem is 1-D and compares isotopic concentrations. In general the average results from MPACT+ORIGEN were comparable to the other numerical results in their agreement to experiment.

The other benchmark, a JAERI benchmark on next generation LWR fuels, analyzed a PWR pin and assembly problem. There was also good agreement in these results. This benchmark does not have a reference, but the MPACT+ORIGEN results were comparable to the other MPACT generated results which fell within the spread of all participants, and not far from the average of the results.

Thus, it was concluded that ORIGEN was successfully integrated into MPACT and is capable of providing reasonably accurate results.

Some additional comparison was done on the average performance and it was found that for the current implementation the point depletion solver in MPACT is approximately 14x faster than ORIGEN. However, the number of nuclides being treated within ORIGEN is about 4x as many as that in MPACT. Additionally, there are some simple optimizations that can be done to the way that ORIGEN was integrated to provide some further performance increase. The suggested target time for a point depletion solve was 0.1 seconds, at present ORIGEN would need to be improved by a factor of 2-3x to achieve this goal. It is believed that this should be achievable provided a smaller depletion chain is used and some other minimal performance tuning is performed.

Other future work will focus on the implementation of other time discretization schemes, specifically the post-correction method, that allow for larger time steps without a loss in accuracy to reduce the overall run time.

REFERENCES

[1] C.E. Sanders and I.C. Gauld, "Isotopic Analysis of High-Burnup PWR Spent Fuel Samples From the Takahama-3 Reactor," NUREG/CR-6798, Oak Ridge National Lab, Oak Ridge, TN, (2003).

[2] A. Yamamoto, et al., "Benchmark problem suite for reactor physics study of LWR next generation fuels," *J. of Nucl. Sci. & Tech.*, **39**, pp. 900-912, (2002).

[3] B. Kochunas, "Advanced Simulations of Heterogeneous Light Water Reactor Cores for Transuranic Recycle," *Master's Thesis*, University of California, Berkeley, Dec. (2008).

[4] B. Collins, et al., "Demonstration of Advanced Pin-Resolved Depletion with MPACT (Rev. 1)," CASL-X-2013-0276-001, University of Michigan, Ann Arbor, MI, Feb. (2014).

[5] Y. Nakahara, et al., "Translation of Technical Development on Burn-up Credit for Spent LWR Fuels," ORNL/TR-2001/01 (JAERI-Tech 2000-071), Oak Ridge National Lab, Oak Ridge, TN, (2002).

[6] *OECD Nuclear Energy Agency SFCOMPO Spent Fuel Isotopic Composition Database*, Organisation for Economic Co-operation and Development, 2011. Web. 27 June 2014. https://www.oecd-nea.org/sfcompo/

[7] K. Okumura, et al. "Benchmark results of burn-up calculation for LWR Next Generation Fuels," *Proc. Int. Conf. The Physics of Fuel Cycles and Advanced Nuclear Systems: Global Developments (PHYSOR2002),* American Nuclear Society, Seoul, Korea, October 7-10, [CD-ROMO] (2002).

[8] T. Kitada, et al. "Analysis of Benchmark Results for Reactor Physics of LWR Next Generation Fuels," *Proc. Int. Conf. The Physics of Fuel Cycles and Advanced Nuclear Systems: Global Developments (PHYSOR2004),* American Nuclear Society, Chicago, IL, USA, April 25-29, [CD-ROMO] (2004).

[9] D.J. Lee, J.D. Rhodes, and K. Smith, "Quadratic Depletion Method for Gadolinium Isotopes in CASMO-5," *J. of Nucl. Sci. & Eng.*, **174**, pp. 79-86, (2013).